A Journal of the Gesellschaft Deutscher Chemiker

Angewandte International Edition

GDCh

Chemie

www.angewandte.org

Accepted Article

Title: Aldolase Cascade by Self Assembled Nanotubes of Short Peptide Amphiphile

Authors: Antara Reja, Syed Pavel Afrose, and Dibyendu Das

To be cited as: *Angew. Chem. Int. Ed.* 10.1002/anie.201914633
Angew. Chem. 10.1002/ange.201914633

Link to VoR: http://dx.doi.org/10.1002/anie.201914633
http://dx.doi.org/10.1002/ange.201914633

WILEY-VCH

10.1002/anie.201914633

WILEY-VCH

COMMUNICATION

Aldolase Cascade by Self Assembled Nanotubes of Short Peptide Amphiphile

Antara Reja, Syed Pavel Afrose and Dibyendu Das*

Abstract: Early evolution benefited from a complex network of reactions involving multiple cascades of carbon-carbon bond formation and breaking that were critical for primitive metabolism. Nature gradually chose highly evolved and complex enzymes such as lyases featuring binding pockets with precise arrangement of amino acids to efficiently foster the forward and reverse steps of this C-C bond cleavage with remarkable selectivity of substrates. We report a lipidated short peptide which accesses homogenous nanotubular morphology to efficiently catalyze the C-C bond cleavage and formation. This system showed morphology-dependent catalytic rates suggesting the formation of a binding pocket and registered enhancements in presence of hydrogen bond donor tyrosine which is exploited by extant aldolases. Notably, these assemblies showed excellent selectivity of substrates and templated the formation of a specific adduct from a pool as a sole product. The ability to catalyze metabolically relevant cascade transformations argues the importance of such systems in early evolution.

Present biology uses a number of highly evolved enzymes in complex chemical networks to achieve the cascade of events required for anabolic and catabolic pathways.[1,2] The remarkable catalytic prowess of such modern enzymes arises from complex three-dimensional structures accessed by long peptide sequence which folds to create binding sites featuring specific residues.[3] Precise arrangement of such residues helps in manipulating protonation events, inducing a charge-transfer relay network to polarize and activate nucleophile or electrophile and so forth. Interestingly, unlike extant enzymes which work on very specific substrates and usually specialize in only one reaction, the primitive catalyst had very broad specificities.[4] Fewer rudimentary enzymes showed promiscuity in the primordial conditions as they were capable of working on multiple substrates, catalyzing forward and reverse steps for the cascade of reactions required for early metabolic capabilities and thus contributed greatly towards enrichment of the chemical inventory.[5] Gradual divergence towards specialized roles of enzymes happened through duplication, mutation and selection which led to the existing diversity of biocatalysts and their role towards increased metabolic efficiency.[6] For instance, modern aldolases act as lyases which use lysine and tyrosine in the binding pockets for selectively catalyzing the forward and the reverse steps of the aldol cascade.[7] Carbon-carbon bond manipulation is critical for diverse reactions, from formose reaction to modern metabolic pathways such as Calvin cycle and glycolysis.[8] We asked whether a short peptide capable of accessing homogenous nanostructures would be able to foreshadow the generation of an enzyme binding pocket and catalyze both the forward and

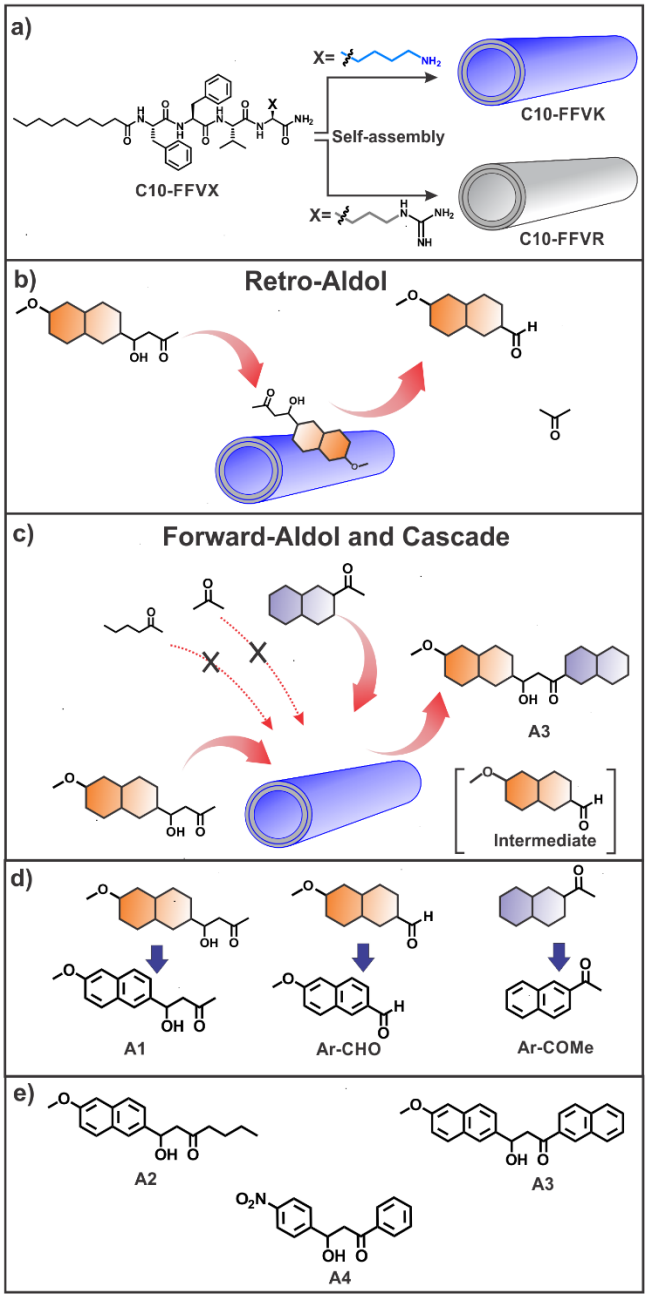

Figure 1. a) Structures of the peptide amphiphiles. b) Schematic representation of retro-aldol reaction with **A1** in presence of nanotube. c) Cascade reaction through bond breaking of adduct **A1**, followed by a selective bond formation in presence of different ketones acting as nucleophiles. The intermediate **Ar-CHO** and final product **A3** are shown. d,e) Elaborated view of symbols with structures of substrates.

[a] Department of Chemical Sciences & Centre for Advanced Functional Materials, Indian Institute of Science Education and Research (IISER) Kolkata, Mohanpur, West Bengal, 741246, India
E-mail: dasd@iiserkol.ac.in

reverse steps of C-C bond cascade transformations.[9] Towards this end, we report self-assembled nanotubes capable of carrying out two of the most critical transformations in extant biology, selective carbon-carbon bond breaking/formation, and importantly directing cascade reactions for specific condensation product distribution.

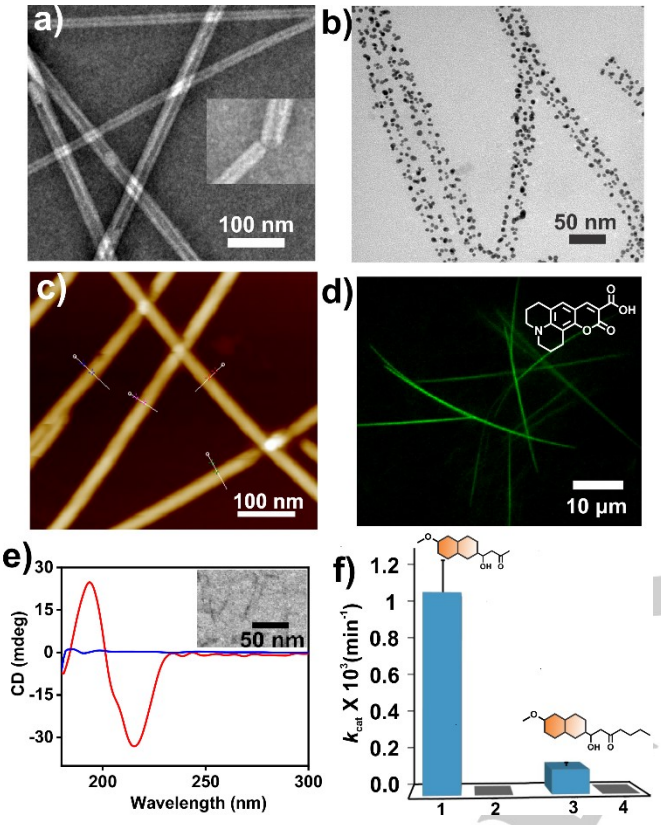

Figure 2. a) TEM image of nanotube (inset: magnified image of nanotube). b) TEM image of negatively charged gold nanoparticle bound with nanotube. c) AFM image of nanotube. d) CLSM image of coumarin 343 dye bound to **C10-FFVK** nanotubes (λ_{ex}=488 nm). e) CD of self-assembled **C10-FFVK** (nanotube) before (red) and after (blue) treatment with HFIP (inset: TEM image of HFIP treated **C10-FFVK** nanotube) f) Retro-aldol rate of **A1** and **A2** by the nanotubes of **C10-FFVK** (blue bars) and **C10-FFVR** (grey bars).

We started with residue 18 to 20 (^{18}VF^{20}F) of the core of Aβ 1-42 sequence which is associated with the protein deposits seen in Alzheimer's disease.[10] To impart colloidal stability, we installed lysine at the C-terminal while the N-terminal was coupled to decanoic acid, yielding the amphiphile **C10-FFVK** (Figure 1a, Figure S1, SI). Transmission electron microscopy (TEM) images of the assemblies showed different morphologies depending on the incubation time. Assemblies aged up to 7-15 days showed mostly nanofiber like structures (Figure S2, SI). Interestingly, on aging for up to 30 days and more, the peptide assemblies accessed homogenous nanotubular structures having a diameter of 23 ± 2 nm with well-defined walls (Figure 2a, S2, SI).[11] Atomic force microscopy done with the 30 days incubated samples also revealed homogenous nanotubular morphologies with heights of 18 ± 2 nm, suggesting a wall thickness of 9 ± 1 nm (Figure 2c, predicted model of assembly in Figure S3, SI). Circular dichroism (CD) spectra showed a negative band at around 220 nm, indicating β-sheet like secondary structure (Figure 2e).[12] The FTIR spectrum of **C10-FFVK** peptide amphiphile showed a strong amide I absorption band at 1613 cm^{-1} (Figure S4, SI). To investigate the nature of the surface, the nanotubes were incubated with negatively charged AuNP. TEM showed ordered binding of nanoparticles on the nanotubes, indicating the presence of solvent exposed arrays of positively charged lysines (Figure 2b). Control done using positively charged AuNP showed no such specific binding (Figure S5, SI). Further, to check the ability of the tubes to bind hydrophobic moieties, we used fluorescent dye coumarin 343 as a model guest. Confocal microscopy showed fluorescent nanostructures with uniform binding of the dye on the tubes, underpinning the ability of the nanotube to bind to small molecules (Figure 2d).

The above experiments suggested the positively charged surface of nanotubes with dense array of lysines that can be exploited for catalyzing reactions via formation of imine intermediate.[6c,13] We investigated whether these nanotubes can catalyze retro-aldol reactions and importantly, whether these can show selectivity among substrates. The two substrates used were methodol (**A1**), the adduct of acetone and fluorescent 6-methoxy-2-naphthaldehyde (**Ar-CHO**) and its more hydrophobic congener (**A2**), an adduct of 2-hexanone with the same aldehyde. The retroaldolase activity was monitored by UV-Vis spectroscopy at pH 7.45 HEPES buffer (10 mM), (Figure S6, S7, S8 see SI for details). Interestingly, the peptide nanotubes showed preference of substrate for the C-C bond cleavage as **A1** cleaved with an order of magnitude higher catalytic activity [k_{cat} = (1.02±0.17)×10^{-3} min^{-1}] than **A2** [k_{cat} = (0.12±0.016)×10^{-3} min^{-1}, Figure 2f]. The reaction progress could also be seen from fluorescence spectroscopy which showed gradual increment of **Ar-CHO** at 452 nm (Figure S9, SI). Further, the reaction was monitored from HPLC analysis. A gradual decrease of peak area of **A1** with simultaneous increase of **Ar-CHO** was observed (Figure S10, SI). Control reaction done with only molecular lysine showed more than 4 order of magnitude lower rates for both the substrates. Interestingly, retro-aldol reactions done in organic solvent THF without nanotubes using tertiarybutylammonium hydroxide as base yielded similar rates for **A1** and **A2** (Figure 3a) suggesting the role of the nanotubular surface in selection among substrates. To find out the reason for the preference of the nanotubes for **A1** over **A2,** we proposed to monitor the binding of the substrates with fluorescence spectroscopy. To circumvent the problem that would arise from the cleaved product (**Ar-CHO**), we mutated lysine with arginine to create a control sequence **C10-FFVR** (Figure 1a). **C10-FFVR** assembled to form morphologically similar nanotubes as seen for **C10-FFVK** (diameter=20± 4 nm**,** Figure S11). As predicted, **C10-FFVR** nanotubes were unable to cleave the substrates **A1** and **A2** even after prolonged incubation (Figure 2f). Notably, **A1** showed a significant enhancement of the fluorescence compared to **A2** (λ_{ex}=290 nm, Figure S12), indicating more binding for **A1** resulting in higher rates.

We further found that the morphology of the assembled peptide had a remarkable role on the activity. Fiber like morphology accessed after ca. 15 days of assembly showed ca. 50 % lower activity compared to the activity seen in case of the matured nanotubes assembled for 30 days (Table S1, SI).[11d, 14] To probe

10.1002/anie.201914633

this, the binding capabilities of **C10-FFVK** based on their states of assembly were investigated. Fluorophore 8-Anilino-1-naphthalenesulfonic acid (ANS), known to report the hydrophobicity of the binding sites of the self-assembled systems, showed significant increase in intensity along with a substantial blue shift in the emission maxima when incubated with the **C10-FFVK** nanotubes (λ_{em}=485 nm, $\lambda_{em(in\ buffer)}$=516 nm).[15] However, for fibers, ANS showed substantially lower fluorescence intensity with lesser extent of blue shift (λ_{em}=489 nm, Figure S13, SI). This suggested stronger binding capability of the nanotubes in comparison to the fibers. Intrinsic fluorescence of **A1** showed a similar trend with the assemblies of the control sequence **C10-FFVR** (Figure S12).

Notably, the fibers had lesser selectivity between the substrates **A1** and **A2** when the ratio of retroaldolase activities was compared with the nanotubes (Figure 3a). This again highlighted the role of a binding surface on the nanotubes which resulted in higher activity with more selectivity. To further investigate the importance of the self-assembled nanotubes and the binding surface generated upon assembly, we treated the nanotubes by hexafluoroisopropanol (HFIP) to disassemble the nanostructures completely and checked the activity within ca. 2 min (See SI for details). The disassembly was confirmed from the loss of CD signal and through TEM (Figure 2e, SI for details). The disassembled peptide amphiphile showed ca. 28 times lower activity with no selectivity when compared to the assembled nanotubes, thus underpinning the role of binding surface for catalysis and selectivity (Figure 3a, Table S1, SI). To probe the binding surface further, we used ANS fluorescence which suggested poor binding of the fluorophore to the disassembled peptides of **C10-FFVK** (Figure S13, SI). Congo Red (CR) binding studies with UV Vis spectroscopy also suggested stronger binding to the nanotubes than fibers and disassembled peptides (Figure S14).[12a]

Extant aldolases elegantly use the H-bond donor capabilities of a proximal tyrosine in the active site to facilitate the C-C bond cleavage. The phenolic –OH group of tyrosine critically assists by proton transfer thus increasing the electrophilicity of the carbonyl group of the substrate prior to formation of the imine. Mutant proteins with phenyl alanine in place of tyrosine results in sharp decline of activity despite the presence of lysine.[13c,d] We asked whether our designed catalytic nanotubes having lysine arrays can show higher activity in presence of tyrosine on its surface. For this purpose, we used **Fmoc-Y** (Figure 3b) which can bind via the hydrophobic interactions, in a similar fashion as seen for coumarin 343. The fluorescence of **Fmoc-Y** in presence of peptide nanotubes showed red shift along with quenching of fluorescence intensity of the fluorenyl moiety and thus suggested binding (Figure S15, SI). Notably, we found a significant enhancement in the reaction rate with **A1** in presence of **Fmoc-Y** which was almost 4.9 times higher [k_{cat} = (4.93±0.48) ×10^{-3} min^{-1}] than the nanotubes without tyrosine (Figure 3b, S6, S16, Table S1, SI). Rate enhancement was seen for **A2** as well when **Fmoc-Y** [k_{cat} = (0.37±0.10) × 10^{-3} min^{-1}] was used (S6, S17, Table S1, SI). For controls, we used Fmoc protected phenyl alanine (**Fmoc-F**) where the phenolic -OH moiety was absent (Figure 3b, Table S1, SI). **Fmoc-F** was unable to enhance the retroaldolase rates (Figure 3b). Further, we designed an additive having the Fmoc-tyrosine moiety where the acidic phenolic proton was substituted

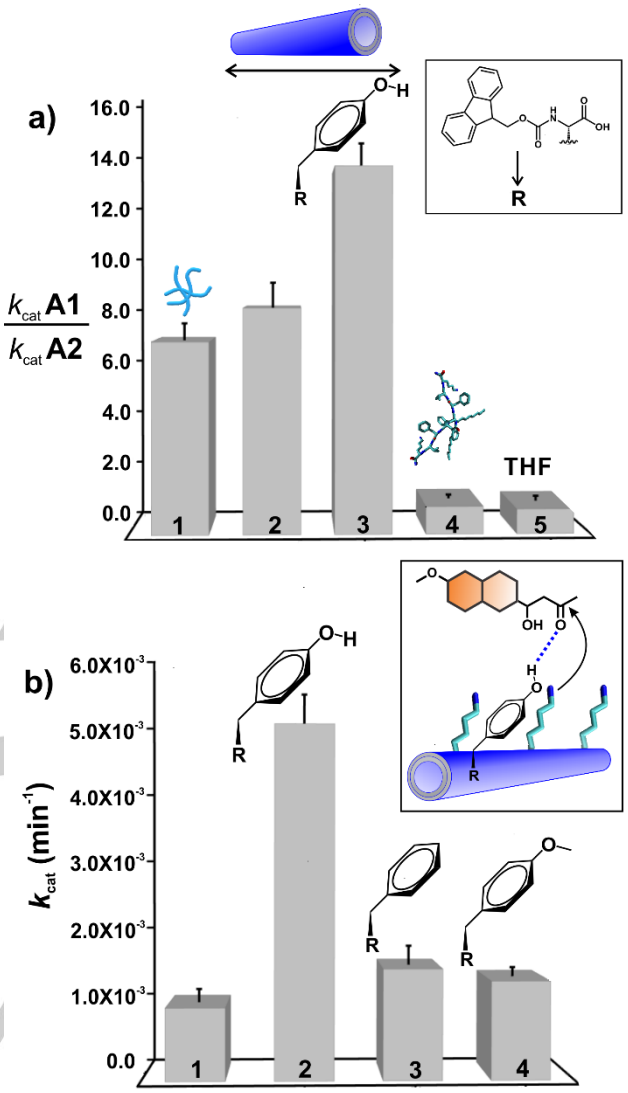

Figure 3. a) Ratio of retro-aldol rates of **A1** vs **A2** catalyzed by 1) fiber 2) nanotube 3) nanotube + **Fmoc-Y** 4) HFIP treated nanotube in buffer and 5) tetrabutylammonium hydroxide in THF. b) Retro-aldol rates of **A1** catalyzed by 1) nanotube and nanotube along with 2) **Fmoc-Y** 3) **Fmoc-F** 4) **Fmoc-Y(OMe)**, and probable mechanism of activation in presence of **Fmoc-Y** (inset).

with methyl group (**Fmoc-Y-OMe**). The lack of the hydrogen bond donor for **Fmoc-Y-OMe** resulted in no enhancement of rate constant for the retro-aldol reaction (Figure 3b, Table S1, SI, Fmoc deprotection was not seen till the course of the reaction, Figure S18, SI).

Aldolases have the ability to catalyze both the forward and the reverse steps of the condensation reaction based on the substrates and hence have profound importance in extant metabolism. We wanted to check whether the designed nanotubes can catalyze the forward aldol as well with the possibility of selectivity. To check the forward activity, reaction mixture containing **Ar-CHO** and acetone was interfaced with the nanotubes. However, no condensation product could be observed

10.1002/anie.201914633

till 48 h. Likewise, a mixture of 2-hexanone with **Ar-CHO** did not yield aldol adduct even after 48 h. At this point we thought of adding an aromatic ketone, 2-acetonaphthone (**Ar-COMe**) to **Ar-CHO** in presence of nanotubes. Notably, we could see generation of the aldol adduct **A3** with time in HPLC (Figure 1). The rate of formation (0.24μM/min) was calculated from HPLC (at 200μM each of **Ar-CHO** and **Ar-COMe**, standard plot of **A3** in Figure S19, SI).

At this point, we were curious to test the capability of the nanotubes to simultaneously perform the forward and reverse aldol and whether these assemblies can promote cascade reactions. For that, we interfaced the nanotubes with mixture of substrates having aldol adduct along with ketones. We started with **A1**, acetone, 2-hexanone and **Ar-COMe**. Expectedly, from HPLC there were three peaks having retention time of 5 min, 11.5 min and 20 min which corresponded to **Ar-COMe**, **C10-FFVK** and **A1** respectively (Figure 4a). After 6 h, a new peak eluted with retention time 15 min which corresponded to the intermediate **Ar-CHO** and simultaneously the absorbance of **A1** peak decreased due to its conversion into **Ar-CHO** (Figure 4a). After 12 h, the decrease of intensity of the **Ar-CHO** and **Ar-COMe** peaks were observed with a gradual elution of a new peak at 22 min (Figure. 4a). Mass spectrometry confirmed the formation of the adduct between **Ar- CHO** and **Ar- COMe** (Figure S20, SI). The rate of formation of the adduct was measured to be 0.07μM/min. To the best of our knowledge, this is the first report of a short peptide-based assembly which can successfully manipulate both the cleavage and formation of the C-C bond for cascade reaction.

Notably, after the generation of the **Ar-CHO**, despite the possibility of formation of multiple adducts in presence of three different ketones, the formation of one adduct underpins the importance of the binding surface. As controls, instead of using

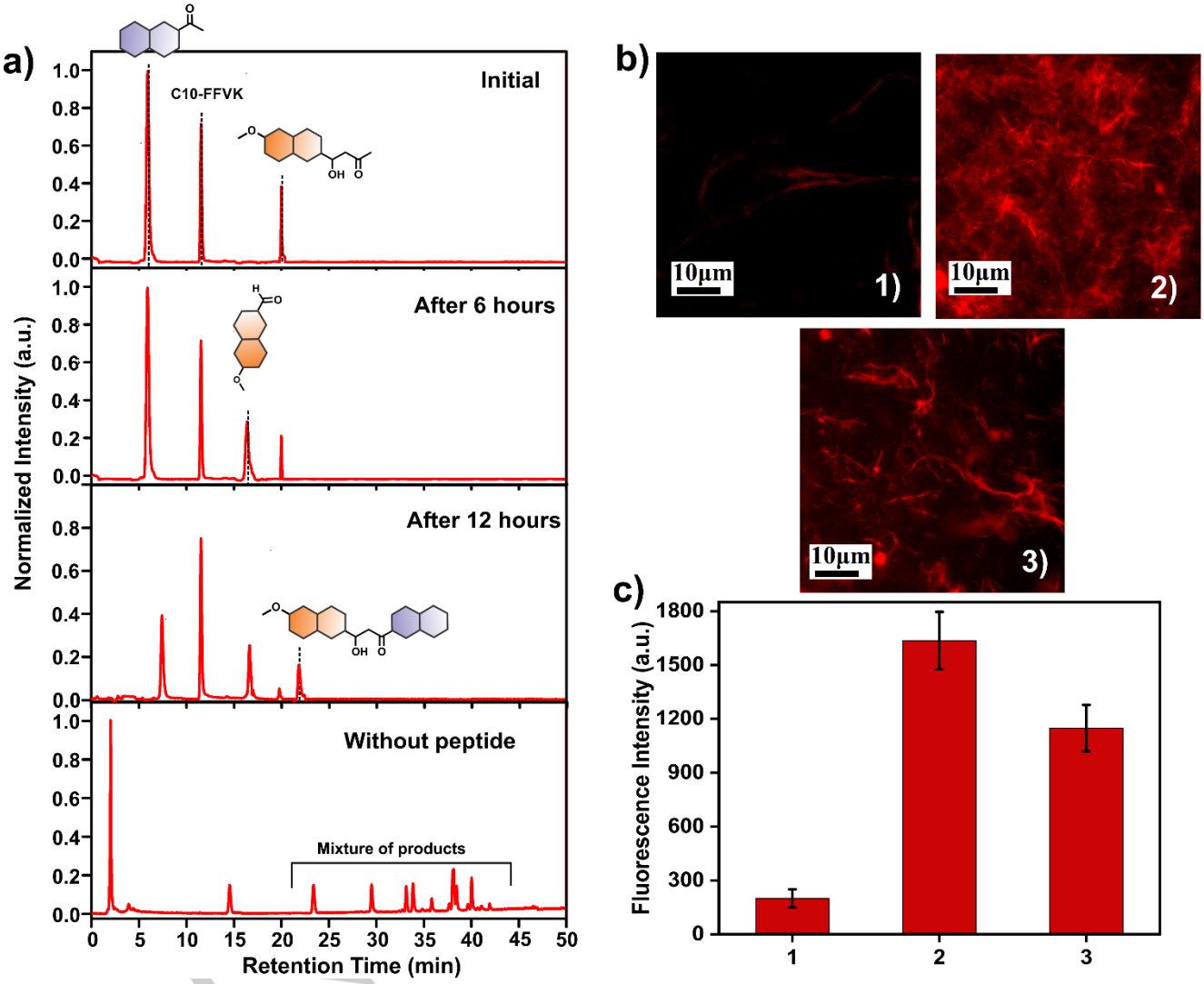

Figure 4. a) HPLC chromatograms of cascade reaction mixture containing **A1**, assembled **C10-FFVK** (nanotube), **Ar-COMe**, 2-hexanone and acetone in 10mM HEPES buffer pH 7.45 with time 1) initial, 2) 6 h, 3) 12 h, and the same reaction mixture in presence of NaOH instead of using nanotube at 12 h (down) b) Representative epifluorescence images to monitor cascade reaction in presence of nanotube at time 1) 30 min, 2) 6 h and 3) 12 h taken in 20 random field of views. c) Intensity profile diagram of same reaction mixture at time 1) 30min, 2) 6 h and 3) 12 h in 20 random field of views to avoid photobleaching.

nanotubes, the one pot reaction was carried out using 1M NaOH. After 12 h, the HPLC analysis of the reaction mixture showed multiple peaks of dehydrated aldol adducts (Figure 4a). Significantly these results suggested that the peptide nanotubes were not only promoting selective aldol adduct formation but importantly impeding the dehydration step in the cascade process. The catalytic ability shown by **C10-FFVK** of templating the forward and retro steps was also monitored through epifluorescence microscopy (Figure. 4b, c). Time resolved epifluorescence microscopy was done with an aqueous buffered solution containing the mixture of **A1**, acetone, 2-hexanone and **Ar-COMe** along with the peptide nanotubes. Twenty random fields of images in triplicate of samples were recorded to rule out the effects of photobleaching (representative images in Figure 4b). Interestingly, gradual emergence of fluorescent nanostructures could be observed. This suggested the formation of fluorescent intermediate **Ar-CHO** over time on the surface of nanotubes. The intensity and density of the fluorescent nanostructures peaked at 6 h. Afterwards, the intensity gradually started to decrease, implying consumption of the intermediate aldehyde due to the ongoing forward aldol reaction on the surface of the nanotubes and subsequent formation of the cascade product **A3**. Control experiment was carried out with peptide nanotubes mixed with **A1**, acetone and 2-hexanone in absence of **Ar-COMe**. This mixture showed only the increase of intensity of fluorescent nanostructures which plateaued after 6 h (Figure S21, SI). The **C10-FFVK** nanotubes were also found to catalyze the cleavage of the adduct **A3** with k_{cat} = (0.072±0.002) X10^{-3} min^{-1} (Figure S23, SI). Finally, to check the capability of the **C10-FFVK** nanotubes to catalyze aldol reactions with other substrates, p-nitrobenzaldehyde and acetophenone were used. The nanotubes could catalyze the formation of their adduct with initial rate of 0.0053±0.0007 μM min^{-1} (**A4**, Figure 1, S24, S25, SI). Also, incubation of **A4** with the nanotubes results in the cleavage with rates of 0.05±0.002 μM min^{-1} as monitored from HPLC (Figure S26, S27, SI).

In conclusion, a short peptide amphiphile which accessed homogenous nanotubular morphologies was shown to catalyze the formation and cleavage of the carbon-carbon bond, two of the most critical transformations for the emergence of metabolism. In analogy to the modern aldolases, these peptide assemblies foreshadowed the generation of a binding pocket as in presence of a bound tyrosine moiety, the activity showed significant enhancement. These functions had a critical dependence on the binding surface of the accessed morphologies as the unassembled building blocks or newly formed fibers were catalytically less proficient. The peptide assemblies further showed selectivity towards specific substrates and importantly demonstrated the capability to direct a cascade reaction with specific distribution of metabolized product which was not dehydrated. Catalyzing selectively the forward and reverse steps of cascade condensation reactions are traits of modern lyases which are critical for metabolism, suggesting that the simple systems such as the reported ones might have had an advantage in early evolution.

Acknowledgements

DD is thankful to SERB (EMR/2017/005126), DST, GOI. AR and SPA acknowledge IISER Kolkata and UGC for fellowships respectively.

Conflict of interest

The authors declare no conflict of interest.

Keywords: Peptide-amphiphile • Self-assembly • Cascade • Retro-aldolase • Catalysis

[1] a) C. R. Woese, *Proc. Natl. Acad. Sci. USA* **2002**, *99,* 8742-8747; b) J. Greenwald, R. Riek, *J. Mol. Biol.* **2012**, *421*, 417-426; c) C. P. J. Maury, *Cell. Mol. Life Sci*. **2018**, *75*, 1499−1507; d) O. Carny, E. Gazit, *FASEB J*. **2005**, *19*, 1051-1055; e) J. T. Goodwin, A. K. Mehta, D. G. Lynn, *Acc. Chem. Res.* **2012**, *45*, 2189-2199; f) J. Greenwald, M. P. Friedmann, R. Riek, *Angew. Chem.* **2016**, *128,* 11781-11785; *Angew. Chem. Int. Ed.* **2016**, *55*, 11609-11613; g) B. Rubinov, N. Wagner, H. Rapaport, G. Ashkenasy, *Angew. Chem*. **2009**, *121*, 6811-6814; *Angew. Chem. Int. Ed.* **2009**, *48*, 6683-6686; h) B. M. Rode, *Peptides*. **1999**, *20*, 773-86; i) J. Greenwald, W. Kwiatkowski, R. Riek, *J. Mol. Biol.* **2018**, *430*, 3735-3750; j) S. K. Rout, M. P. Friedmann, R. Riek, J. Greenwald, *Nat. Commun*. **2018**, *9*, 234; k) J. E. Smith, A. K. Mowles, A. K. Mehta, D. G. Lynn, *Life* **2014**, *4*, 887-902.

[2] a) J. A. Bradford, K. A. Dill, *Proc. Natl. Acad. Sci. USA* **2007**, *104*, 10098-10103; b) J. Nanda, B. Rubinov, D. Ivnitski, R. Mukherjee, E. Shtelman, Y. Motro, Y. Miller, N. Wagner, R. C. Luria, G. Ashkenasy, *Nat. Commun.* **2017**, *8*, 434; c) A. Walther, *Adv. Mater.*, DOI: 10.1002/adma.201905111.

[3] a) R. Riek, D. S. Eisenberg, *Nature* **2016**, *539*, 227-235; b) Q. Wang, Z. Yang, L. Wang, M. Ma, B. Xu, *Chem. Commun*. **2007**, *0*, 1032-1034; c) T. M. Hermans, *Nat. Nanotechnol*. **2016**, *11*, 920−921; d) D. Zaramella, P. Scrimin, L. J. Prins, *J. Am. Chem. Soc.* **2012**, *134*, 8396 – 8399.

[4] a) R. C. Rodrigues, C. Ortiz, Á. Berenguer-Murcia, R. Torres, R. Fernández-Lafuente, *Chem. Soc. Rev.* **2013**, *42*, 6290−6307; b) R. E. Parales, K. Lee, S. M. Resnick, H. Jiang, D. J. Lessner, D. T. Gibson, *J. Bacteriol*. **2000**, *182*, 1641-1649; c) T. P. Knowles, R. Mezzenga, *Adv. Mater*. **2016**, *28*, 6546–6561.

[5] a) J. M. Berg, J. L. Tymoczko, L. Stryer, *Biochemistry*, *5th ed.,* New York, **2002**; b) J. Ottelé, A. S. Hussain, C. Mayer, S. Otto, *ChemRxiv Preprint*, **2019** https://doi.org/10.26434/chemrxiv.10002032.v1; c) X. Zhao, H. Palacci, V. Yadav, M. M. Spiering, M. K. Gilson, P. J. Butler, H. Hess, S. J. Benkovic, A. Sen, *Nat. Chem.* **2017**, *10*, 311-317; d) J. H. van Esch, R. Klajn, S. Otto, *Chem. Soc. Rev*. **2017**, *46*, 5474-5478.

[6] a) M. O. Guler, S. I. Stupp, *J. Am. Chem. Soc.* **2007**, *129*, 12082-83; b) C. Zhang, X. Xue, Q. Luo, Y. Li, K. Yang, X. Zhuang, Y. Jiang, J. Zhang, J. Liu, G. Zou, X.-J. Liang, *ACS Nano* **2014**, *8*, 11715−11723; c) T. O. Omosun, M. C. Hsieh, W. S. Childers, D. Das, A. K. Mehta, N. R. Anthony, T. Pan, M. A. Grover, K. M. Berland, D. G. Lynn, *Nat. Chem*. **2017**, *9*, 805-809; d) M. Tena-Solsona, J. Nanda, S. Diaz-Oltra, A. Chotera, G. Ashkenasy, B. Escuder, *Chem. Eur. J*. **2016**, *22*, 6687–6694; e) S. Bal, K. Das, S. Ahmed, D. Das, *Angew. Chem. Int. Ed.* **2019**, *58*, 244-247; *Angew. Chem. 131*, 15930-15934; f) C. Q. Zhang, R. Shafi, A. Lampel, D. MacPherson, C. G. Pappas, V. Narang, T. Wang, C. Maldarelli, R. V. Ulijn, *Angew. Chem. Int. Ed.* **2017**, *56*, 14511–14515; *Angew. Chem.* **2017**, *129*, 14703-14707; g) S. P. Afrose, S. Bal, A. Chatterjee, K. Das, D. Das, *Angew. Chem. Int. Ed.* **2019** *58*, 15783–15787; *Angew. Chem.* **2019**, *131*, 15930-15934; h) C. M. Rufo, Y. S. Moroz, O. V. Moroz, J. Stçhr, T. A. Smith, X. Hu, W. F. DeGrado, I. V. Korendovych, *Nat. Chem*. **2014**, *6*, 303–309; i) S. Ahmed, A. Chatterjee, K. Das, D. Das, *Chem. Sci*. **2019**, *10*, 7574 – 7578.

[7] a) C. Zeymer, R. Zschoche, D. Hilvert, *J. Am. Chem. Soc.* **2017**, *139*, 12541−12549; b) A. Romero-Rivera, M. Garcia-Borràs, S. Osuna, *ACS*

Catal. **2017**, *7*, 8524−8532; c) S. Junker, R. Roldan, H.-J. Joosten, P. Clapés, W.-D. Fessner, *Angew. Chem. Int. Ed*. **2018**, *57*, 10153−10157; d) J. W. Schafer, I. Zoi, D. Antoniou, S. D. Schwartz, *J. Am. Chem. Soc*. **2019**, *141*, 10431−10439; e) K. Hernandez, J. Bujons, J. Joglar, S. J. Charnock, P. D. de María, W. D. Fessner, P. Clapés, *ACS Catal.* **2017**, *7*, 1707– 1711.

[8] E.Szathmáry, *Philos. Trans. R. Soc. Lond. B Biol. Sci.* **2007,** *362*, 1781–1787.

[9] a) N. Kapil, A. Singh, D. Das, *Angew. Chem. Int. Ed.* **2015**, *54*, 6492–6495; *Angew. Chem.* 2015, **127**, 6592– 6595; b) G. Wei, Z. Su, N. P. Reynolds, P. Arosio, I. W. Hamley, E. Gazit, R. Mezzenga, *Chem. Soc. Rev*. **2017**, *46*, 4661–4708; c) R. P. Cheng, S. H. Gellman, W. F. DeGrado, *Chem. Rev.* **2001**, *101*, 3219; d) B. Saha, A. Chatterjee, A. Reja, D. Das, *Chem. Commun.* **2019**, DOI: 10.1039/c9cc07358b; e) A. R. Hirst, S. Roy, M. Arora, A. K. Das, N. Hodson, P. Murray, S. Marshall, N. Javid, J. Sefcik, J. Boekhoven, J. H. van Esch, S. Santabarbara, N. T. Hunt, R. V. Ulijn, *Nat. Chem*. **2010**, *2*, 1089-1094; f) N. Kapil, A. Singh, M. Singh, D. Das, *Angew. Chem. Int. Ed*. **2016**, *55*, 7772– 7776; *Angew. Chem*. **2016**, *128*, 7903– 7907; g) Y. Gao, F. Zhao, Q. Wang, Y. Zhang, B. Xu, *Chem. Soc. Rev*. **2010**, *39*, 3425-3433; h) M. Tena-Solsona, J. Nanda, S. Diaz-Oltra, A. Chotera, G. Ashkenasy, B. Escuder, *Chem. Eur. J*. **2016**, *22*, 6687–6694.

[10] M. P. Murphy, H. LeVine III, *J. Alzheimer's Dis*. **2010**, *19*, 311-23.

[11] a) C. Seuring, J. Verasdonck, P. Ringler, R. Cadalbert, H. Stahlberg, A Böckmann, B. H. Meier, R. Riek, *J. Phys. Chem. B* **2017**, *121*, 1783-1792; b) K. Lu, J. Jacob, P. Thiyagarajan, V. P. Conticello, D. G. Lynn, *J. Am. Chem. Soc*. **2003**, *125*, 6391–6393; c) J. Adamcik, R. Mezzenga, *Angew. Chem., Int.* Ed. **2018**, *57*, 8370-8382; *Angew. Chem.* **2018**, *130*, 8502–8515; d) J. K. Sahoo, C. G. Pappas, I. R. Sasselli, Y. M. Abul-Haija, R. V. Ulijn, *Angew. Chem. Int. Ed*. **2017**, *56*, 6828–6832; *Angew. Chem*. **2017**, *129*, 6932–6936; e) M. Colomb-Delsuc, E. Mattia, J. W. Sadownik, S. Otto, *Nat. Commun*. **2015**, *6*, 7427; f) J. Li, Z. Zhan, X. Du, J. Wang, B. Hong, B. Xu, *Angew. Chem. Int. Ed*. **2018**, *57*, 11716–11721; *Angew. Chem*. **2018**, *130*, 11890–11895; g) A. K. Mehta, K. Lu, W. S. Childers, S. Liang, J. Dong, J. P. Snyder, S. V. Pingali, P. Thiyagarajan, D. G. Lynn, *J. Am. Chem. Soc.* **2008**, *130*, 9829-9835; h) A. Reja, A. Biswas, J. Yadav, D. Dev, A. K. Das, *ChemistrySelect*, **2017**, *2*, 10984-10989. i) J. P. Schneider, D. J. Pochan, B. Ozbas, K. Rajogopal, L. Pakstis, J. Kretsinger, *J. Am. Chem. Soc*. **2002**, *124*, 15030-15037; i) G. M. Whitesides, B. Grzybowski, *Science* **2002**, *295*, 2418-2421.

[12] a) W. S. Childers, A. K. Mehta, K. Lu, D. G. Lynn, *J. Am. Chem. Soc*. **2009**, *131*, 10165–10172; b) W. F. DeGrado, J. P. Schneider, Y. Hamuro, *J. Pept. Res.* **1999**, *54*, 206-217.

[13] a) L. Jiang, E. A. Althoff, F. R. Clemente, L. Doyle, D. Röthlisberger, A. Zanghellini, J. L. Gallaher, J. L. Betker, F. Tanaka, C. F. Barbas III, D. Hilvert, K. N. Houk, B. L. Stoddard, D. Baker, *Science* **2008**, *319*, 1387–1391; b) J. K. Lassila, D. Baker, D. Herschlag, *Proc. Natl. Acad. Sci. USA* **2010**, *107*, 4937–4942; c) R. Obexer, A. Godina, X. Garrabou, P. R. E. Mittl, D. Baker, A. D. Griffiths, D. Hilvert, *Nat. Chem.* **2016**, *9*, 50−56; d) S. Schneider, T. Sandalova, G. Schneider, G. A. Sprenger, A. K. Samland, *J. Biol. Chem*. **2008**, *283*, 30064–30072.

[14] J. Shi, G. Fichman, J. P. Schneider, *Angew. Chem. Int. Ed*. **2018**, *57*, 11188–11192; *Angew.Chem*. **2018**, *130*, 11358–11362.

[15] W. G. Gonzalez, J. Miksovska, *Biochim Biophys Acta*, **2014**, *1844*, 1472–1480.

10.1002/anie.201914633

WILEY-VCH

Entry for the Table of Contents (Please choose one layout)

Layout 1:

COMMUNICATION

Aldolase Cascade: Amyloid like lipidated peptide nanotubes have been shown to demonstrate aldolase cascade activity with selectivity. Nanotubes having lysines as exposed residues bind to tyrosine to create an efficient catalyst to show aldolase activity.

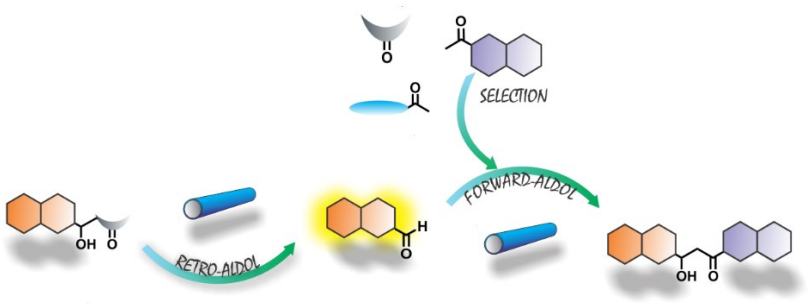

*Antara Reja, Syed Pavel Afrose and Dibyendu Das**

Page No. – Page No.
Aldolase Cascade by Self Assembled Nanotubes of Short Peptide Amphiphile